Nano Today 46 (2022) 101581

Contents lists available at ScienceDirect

Nano Today

journal homepage: www.elsevier.com/locate/nanotoday

Hazard identification of nanomaterials: *In silico* unraveling of descriptors for cytotoxicity and genotoxicity

Naouale El Yamani[a], Espen Mariussen[a,b], Maciej Gromelski[c], Ewelina Wyrzykowska[c], Dawid Grabarek[c], Tomasz Puzyn[c,d], Speranta Tanasescu[e], Maria Dusinska[a], Elise Rundén-Pran[a,*]

[a] Health Effects Laboratory, Department of Environmental Chemistry, NILU - Norwegian Institute for Air Research, 2007 Kjeller, Norway
[b] Norwegian Institute of Public Health, Department of Air Quality and Noise, 0456 Oslo, Norway
[c] QSAR Lab Ltd, Trzy Lipy 3, 80–172, Poland
[d] Laboratory of Environmental Chemoinformatics, Faculty of Chemistry, University of Gdańsk, Wita Stwosza 63, 80-308 Gdansk
[e] Institute of Physical Chemistry "Ilie Murgulescu" of the Romanian Academy, 060021 Bucharest, Romania

ARTICLE INFO

Article history:
Received 9 December 2021
Received in revised form 6 June 2022
Accepted 30 July 2022
Available online xxxx

Keywords:
Nanoparticles
Similarity analysis
Cheminformatics modeling
Physicochemical parameters
DNA damage

ABSTRACT

Hazard identification and safety assessment of the huge variety of nanomaterials (NMs), calls for robust and validated toxicity screening tests in combination with cheminformatics approaches to identify factors that can drive toxicity. Cytotoxicity and genotoxicity of seventeen JRC repository NMs, derived from titanium dioxide, zinc oxide, silver and silica, were tested *in vitro* using human lung alveolar epithelial cells A549. Cytotoxicity was assessed with the AlamarBlue (AB) and colony forming efficiency (CFE) assays, and genotoxicity by the enzyme-linked version of the comet assay. Nanoparticle tracking analysis (NTA) was used to measure size of the NMs in stock and in cell culture medium at different time points. Categorization and ranking of cytotoxic and genotoxic potential were performed (EU-NanoREG2 project approach). Descriptors for prediction of NMs toxicity were identified by quantitative structure-activity relationship (QSAR) analysis. Our results showed that ZnO NMs (NM-110 and NM-111), and Ag NMs (NM-300K and NM-302) were cytotoxic, while the TiO_2 and SiO_2 NMs were non-cytotoxic. Regarding genotoxicity, TiO_2 NM-100, ZnO NM-110, SiO_2 NM-203 and Ag NM-300K were categorized as positive. Cheminformatics modeling identified electron properties and overall chemical reactivity as important descriptors for cytotoxic potential, HOMO-LUMO energy parameter, ionization potential, pristine size for the NMs´ genotoxic potential, and presence of surface coating as descriptor for induction of DNA oxidized base lesions.

Introduction

Nanotechnology has brought significant improvements to our lives. However, the escalation in the production and applications of engineered nanomaterials (NMs) has raised concerns about their safety and potential negative effects on human health and the environment. There is a need for science-based human hazard identification, characterization, risk assessment and risk governance of NMs [1] and for considerations on how hazard and risk are modified along the value chain (from design to successful use in products) and throughout the life cycle (from pristine NMs to disposed or fragmented/aged product) [2]. In addition, for the nanosafety field to follow up on the rapidly growing number of NMs for commercial use, development of time and cost-effective high-throughput (HTP) *in vitro* test methods is important [3]. Nanosafety research and human hazard identification and characterization have been significantly facilitated by use of reliable and predictive new approach methodologies (NAMs), based on advanced *in vitro* and *in silico* methods, in compliance with the 3Rs principle to reduce, refine and replace animal studies. Some advanced *in vitro* models are available for immediate implementation, while many still require validation [2,4]. Further, the safer-by-design (SbD) approach, whereby toxicity testing is performed in parallel with nanotechnology to guide development of smart and safe NMs, is fundamental for sustainable nanotechnology. Toxicity of NMs is closely connected with physicochemical properties, such as size, shape, surface coating and charge. Thus, toxicity testing supported by *in silico* modeling (e.g., quantitative structure–activity relationships [QSAR]) is important to

* Corresponding author.
E-mail address: Erp@nilu.no (E. Rundén-Pran).

https://doi.org/10.1016/j.nantod.2022.101581
1748-0132/

identify physicochemical descriptors that can predict human hazards and facilitate a SbD approach for NMs. Within the H2020 NanoREG2 project, such an approach was trialed for nanosafety assessment, building on the test methods developed and validated within different projects, including the FP7 project NANoREG. The grouping concept aims to facilitate hazard assessment by read-across of toxicological properties to predict toxicity of chemically similar NMs [2,5]. Various regulatory frameworks exist to enable practical application of the grouping and read-across concept. According to EU Regulation on Registration, Evaluation, Authorization and Restriction of Chemicals (REACH) [6], grouping and read-across are among the most commonly used alternative approaches [2]. Recently, a detailed regulatory framework has been developed in greater detail within the GRACIOUS project [5] following regulatory recommendation as described and proposed by the European Chemicals Agency (ECHA) [7–9], where they also made use of previous tools such as DF4nanoGrouping [10,11]. The use of harmonized data storage systems, databases and cloud platforms, for both physicochemical properties and human-toxicity data of NMs is of a great support to the grouping and read-across approach. Such storage systems greatly supports the principles of findability, accessibility, interoperability, and reusability (FAIR) of data. In compliance with this, a major effort was made by establishing the eNanoMapper database within the EU NanoREG2 project, and which later has been extended with data from several EU-funded projects, such as the H2020 RiskGONE project [12].

The use of an integrated approach combining *in vitro* experimental and *in silico* studies has been shown to be of value in identifying hazards and descriptors for toxicity associated with NMs and to give support where crucial empirical information is lacking. During the NanoREG2, several conventional approaches using quantitative (e.g., IC_{50} values) and/or qualitative visualization of data (e.g., Heatmaps) to collect and integrate large and variable sets of data generated by the *in vitro* studies were tested. However, these approaches to identify relevant and experimental factors for NMs similarity analysis seemed to have certain limitations. An approach based on scoring and categorization of NMs´ toxicological responses was applied as described in the NanoREG2 deliverable 1.7 [13]. The approach allows comparison of responses across materials, test methods and cell models. The system was inspired by the EU FP7 project NanoSolutions**.** The integrated approach combining *in vitro* experimental and *in silico* (cheminformatics) studies is based on determining the link between the physicochemical parameters of NMs and the toxicity. Both unsupervised (Principal Component Analysis (PCA) and 2D-Hierarchical Cluster Analysis (2D-HCA)) and supervised (random forest) machine learning techniques based on computational analysis are available [14]. The physicochemical properties of NMs are a determining factor for cellular uptake, fate and toxicity. The primary physicochemical properties include for instance size, composition, surface properties, crystallinity, agglomeration, aggregation, and coating [15–18].

The presented work is part of the completed FP7 project NANoREG, and the H2020 project NanoREG2. In total, seventeen NMs derived from titanium dioxide (TiO_2), zinc oxide (ZnO), silver (Ag) and silica (SiO_2), were tested for cytotoxic and genotoxic potential on human lung epithelial A549 cells, along with analyses for size and size distribution in dispersion as well as in culture medium. To elucidate the cytotoxic potential of these NMs, we applied the colorimetric AlamarBlue (AB) assay and the non-colorimetric colony forming efficiency (CFE) assay. Potential genotoxicity was tested by the minigel version of the comet assay (CA), the method of choice for screening DNA damage in single cells [3]. While the standard comet assay detects strand breaks, we applied a modification involving digestion with a lesion-specific endonuclease, formamidopyrimidine DNA glycosylase (Fpg), to enable also detection of oxidized base lesions, mainly 8-oxoguanine [19]. The possibility of interference of NMs with read-outs of test methods is a serious concern when investigating NMs, and this was addressed in our studies. A strategy to increase robustness and reduce variability when testing NMs for their cytotoxic and genotoxic potential has been published by EL Yamani *et al.* [20]. The testing strategy was based on procedures developed within the FP7 project NANoREG, aiming to develop testing strategies for NMs that can be built into a hazard assessment and regulatory framework.

The selection of these four groups of NMs was based on data completeness and with the intention to be able to identify factors that can drive toxicity and thus to develop and support mechanistic hypotheses. In this work, we have successfully applied the scoring and categorization system to these NMs based on their cytotoxicity and genotoxicity. The applied computational analysis 2D-HCA and PCA identified several factors which may explain their potential toxicity.

Materials and methods

Chemicals

Most reagents for cell culturing were purchased from Sigma-Aldrich; culture medium, fetal bovine serum (FBS), antibiotics and other chemicals used for cell cultivation. SYBRGold® DNA stain was purchased from Invitrogen (Life Technologies™, USA).

Nanomaterials

The NMs investigated are reference materials from the JRC repository, except NM-112 and NM-113 which were from Fraunhofer (Institute for Molecular Biology and Applied Ecology, Aachen, Germany). The NMs tested within the NANoREG and NanoREG2 projects were TiO_2 anatase (NM-100, NM-101, NM-102); TiO_2 rutile (NM-103, NM-104) and NM-105 which is a mix of anatase (85 %) and rutile (15 %) [21], ZnO (NM-110, NM-111, NM-112 and NM-113) [22] and amorphous SiO_2 (NM-200, NM-201, NM-202, NM-203 and NM-204) [23]. In addition, Ag (NM-300K [24] and NM-302 [25,26]) were purchased dispersed in Tween20/polyethylene glycol (PEG). The listed NMs are representative materials used in the testing program of the Organization for Economic Cooperation and Development (OECD) Working Party on Manufactured NMs (WPMN) [27]. Details of all the tested NMs are summarized in Table S1.

Presence of endotoxin contamination of TiO_2 NM-100, 101, 103, ZnO NM-110, 111, SiO_2 NM-200, 203 and Ag NM-300K, 302 was already investigated and results reported in NANoREG Deliverable 5.06 [28]. All particles tested, except for NM-110 (uncoated ZnO particles), showed no direct inflammation-inducing effect using the whole blood assay, as compared to the positive control (lipopolysaccharide (LPS) 2.5 ng/ml), Also, it has been reported in the deliverable that several NMs had little to no effect on the LPS capacity of inducing IL-1β production (namely NM-100, NM-103, NM-200, NM-300K and NM-302) while a few had some enhancing effect (NM-101, NM-110, NM-203, the latter very pronounced). On the other hand, one NM had an appreciable inhibitory effect, namely NM-111 (ZnO particles with a triethoxicaprylsilane coating) [28].

Physicochemical characterization of the NMs dispersions

The NMs were characterized within the course of the EU projects NANOGENOTOX, NANoREG and NanoREG2 (Table S1). Here, the hydrodynamic size and size distribution of the NM-dispersions were analysed *in situ* in stock dispersion and in cell culture medium (before, during and after the exposure) by nanoparticle tracking analysis (NTA) using NanoSight NS500 (Malvern Instruments), that enables measurement of the size of particles from about 30 nm to 1 μm [29]. The instrument combines laser light scattering

microscopy with a charge-coupled device (CCD) camera, which visualizes and records nanoparticles in dispersion. The software identifies nanoparticles moving under Brownian motion and relates the movement to the particle size according to the Stoke-Einstein equation.

Preparation of NM dispersions

A stock of each NM (except Ag NM-300K and Ag-NM-302 which were purchased dispersed) was prepared at 2.56 mg/ml by pre-wetting in 0.5 % absolute ethanol before suspending in 0.05 % bovine serum albumin (BSA) in MilliQ water. The suspension was sonicated using probe sonicator (Labsonic P, 3 mm probe, form Sartorius Stedim Biotech, Göttingen, Germany) at 50 % amplitude for 15 min on ice. The sonicator was previously calibrated, following the NANOGENOTOX protocol [30] to determine the adequate setting to achieve an acoustic power of 7.35 ± 0.05 W. After sonication, the resulting stock dispersion was serially diluted to achieve a logarithmic range of concentrations from 0.01 to 100 μg/cm^2 before exposure of the cells (considering the surface area of the 96-well plate format of 0.32 cm^2). Prior to cell exposure and within 30 min from the end of sonication, a sample from each NM dispersions was characterized for size and size distribution by the NTA. The cells were then exposed within approximately 1 hour (h) after preparation of the dispersion.

Cell cultivation and exposure to NMs

The human lung epithelial cell line A549 was kindly provided by GAIKER within the common NANoREG project so that each partner would work with the same batch of cells. Cells were cultivated in 75 cm^2 culture flasks in Dulbecco´s modified Eagle medium (DMEM, Sigma) supplemented with 9 % fetal bovine serum (FBS) and penicillin (100 U/ml) and streptomycin (100 μg/ml) in a CO_2 incubator at 37 °C.

For the AB and comet assays, the day before exposure the cells (passage 3, 4, 9 and 12) were trypsinised and 1 × 10^4 cells were seeded into each well of 96-well plates. Cell density was measured by an automatic cell counter (Invitrogen). The cells were exposed in duplicate to increasing concentrations of NMs for 3 or 24 h in a total volume of 200 μl per well.

For the CFE assay, the cells were seeded at 50 cells/well in 6-well plates, in a volume of 2 ml of cell culture medium per well, 1–2 h before exposure. On the day of treatment, the cells were exposed to each of the NMs at different concentrations; cytotoxicity was measured using AB and CFE assays, and genotoxicity using the enzyme-linked version of the comet assay. The negative control was culture medium, and the positive control was either hydrogen peroxide H_2O_2 (1 mM, 3 h exposure) or chlorpromazine (CHL) at 50 μl for the AB assay, or Staurosporin (STS) at 10 nM or CHL at 50 μM for the CFE assay. The NM-300K (1 or 10 μg/cm^2) was also applied as a positive reference NM for the CFE experiments within NanoREG2. The corresponding dispersant solutions of NM-300K and NM-302 were included as solvent controls for these particles.

For the AB and comet assay, each material was subjected to three or four independent experiments, with duplicate exposure wells within each experiment. For the CFE assay, each material was tested in six replicate wells within each experiment, and in three independent experiments.

Cytotoxicity testing by the AlamarBlue assay

The AB assay assesses cell viability by the metabolic activity of living cells through a colorimetric response due to conversion of resazurin (oxidized form) to resorufin (reduced form), resulting in change from the non-fluorescent and blue resazurin into the highly fluorescent and pink resorufin. The A549 cells were exposed to the NMs in duplicate wells for 3 or 24 h as described [20,31]. After exposure, the cells were washed twice with pre-warmed PBS. Cells were then incubated for 3 h with fresh culture medium supplemented with 10 % AB, after which 40 μl of medium from each well was transferred to a 96-well black polystyrene microplate (four replicate wells). The fluorescence (excitation 530 nm, emission 590 nm) was measured using a FLUOstar OPTIMA microplate reader. To check for interference with the read-out, cell-free wells were exposed to the same range of NMs and incubated with AB solution for the same time as the samples with cells. No interference was found between the NMs tested and the AB readings.

Cytotoxicity testing by the colony forming efficiency assay

The CFE assay is a label-free method based on cell proliferation and survival, quantifying colony formation. The CFE assay was optimized and standardized for NM testing, validated in an inter-laboratory comparison, and shown to be sufficiently sensitive to detect potential NM toxicity [32,33]. We modified the assay for higher throughput by reducing the number of cells to 50 per well and applying a 6-well plate format, as described by El Yamani *et al.* [20]. The test allows detection of cytotoxic effects (reduction in number of colonies) as well as cytostatic effects (reduction in colony area – number of cells). The A549 cells were plated out in small inocula and exposed as described above. When colonies were clearly visible after 9–12 days, they were stained with 1 % methylene blue for 1–2 h, the plates rinsed with water, dried and the colonies counted manually using an e-count pen. Three independent CFE assays were performed for each NM. The relative CFE (rCFE) was calculated relative to the unexposed control (NC) (set to 100 %).

Genotoxicity testing by the comet assay

The enzyme-linked version of the comet assay was performed as described [20,31,34]. Briefly, A549 cells were seeded in 96-well plates (1 × 10^4 cells /well) 24 h before exposure. On the day of exposure, the cells were exposed to freshly dispersed NMs for 3 or 24 h. Depending on the results of the cytotoxicity tests, the highest concentrations were in some cases omitted. At the end of exposure, the cells were washed with PBS, trypsinised and re-suspended in medium. Approximately 0.5 × 10^4 cells were transferred to a 96-well plate and mixed with three times volume of low melting point (LMP) agarose (0.8 % in PBS) at 37 °C. Drops of 10 μl were placed on previously pre-coated glass slides (0.5% normal melting point agarose). In our set-up, we used the format of 12-gels per slide, with 2 gels per concentration. After 5 min at 4 °C, the slides were immersed into cold lysis solution (2.5 M NaCl, 0.1 M EDTA, 10 mM Tris, 10 % Triton X-100, pH 10) and incubated overnight. After lysis, slides were placed in cold alkaline solution (0.3 M NaOH, 1 mM EDTA) and incubated for 20 min, followed by electrophoresis at 1.25 V/cm for 20 min in a horizontal electrophoresis tank. Slides were then washed twice in PBS followed by water and allowed to dry.

For visualization, the gels were stained with SYBRGold® (Invitrogen) diluted at 1 μl/ml in Tris-EDTA buffer (10 mM Tris–HCl, 1 mM Na_2-EDTA, pH 7.5–8), covered with a coverslip and examined under a fluorescence microscope (Leica DMI 6000 B). Images of comets were scored using Comet Assay IV software (Perceptive Instruments), calculating median % DNA in tail from 50 comets per gel as a measure of DNA strand breaks (SB).

For DNA base oxidation detection, a modified version of the comet assay protocol was applied by inclusion of a post-lysis incubation with Fpg that recognizes oxidized purines, which are converted to strand breaks [35]. After lysis, the slides were washed twice with Fpg buffer (40 mM HEPES, 0.1 M KCl, 0.5 mM EDTA, 0.2 mg/ml BSA, pH 8.0) before incubation for 30 min at 37 °C in a

humidified box with Fpg diluted in the Fpg-buffer. At the end of the enzyme incubation, the slides were transferred into alkaline electrophoresis buffer and processed from this point as described above.

All experiments included positive and negative controls. As positive control for strand breaks (SB), cells were treated with H_2O_2 (100 μM in PBS), for 5 min at 4 °C. As positive and negative controls for the Fpg assay, we used aliquots of cells previously made and stored frozen at − 80 °C, from a single batch of cells, either untreated, or with a known amount of 8-oxoguanine induced by incubating cells with the photosensitizer Ro19–8022 (Hoffmann La Roche) at 2 μM in PBS and irradiated with visible light (500 W halogen source, 30 cm from cells) for 5 min on ice. Due to the unique physicochemical properties and increased reactivity of nanoparticles, we followed the approach described by Magdolenova *et al.* [36] to check for possible interference of the tested NMs with the assay; briefly the highest concentration of each NM tested was mixed directly with a sample of cells from the negative control just before embedding with agarose. The slides were handled in parallel to the other slides as described above. Net Fpg-sensitive sites were estimated by subtracting the % DNA in tail after lysis only from the % DNA in tail after incubation with Fpg.

Toxicity scoring system and categorization

A scoring system was followed within the NanoREG2 project to assess cytotoxic and genotoxic effects. It is a cumulative system which in the case of the cytotoxicity endpoint takes into account the cytotoxicity value for the maximum concentration tested and the value of EC_{50} (NanoREG2 deliverable 1.6). For the scoring and categorization of NM genotoxicity (SB) and oxidative stress (indicated by oxidatively damaged DNA) endpoints using the enzyme-linked version of the comet assay, the system, including definition of acceptance criteria, was followed as agreed within the NanoREG2 project [13] with some modifications. The NMs were categorized based on scoring of cytotoxicity (Tables 1, 2) and genotoxicity (Table 3). If cytotoxicity at the highest concentration was 20 % relative to the NC (100 %), 1 point was given, and if toxicity reached 50 %, 2 points were given, and so on. If EC_{50} was calculated to be below 100 μg/ml, 2 points were given, a further 2 points if below 60 μg/ml and so on, and the maximum score that could be obtained was then 9. The NMs were categorized as (1) non-toxic (2) slightly toxic and (3) toxic, based on cumulative scores of 0–1, 2–5 and 6–9 respectively. The genotoxic effect was subjected to statistical analysis and the criteria for positive response were a significant concentration-response relationship and at least one concentration significantly different from negative control, or at least two concentrations with a significantly increased frequency of SB or DNA oxidation lesions compared with negative control (Table 3).

Modeling of effect and physicochemical characteristics

In the next step we explored possible relationships between the observed endpoints (cytotoxicity and genotoxicity) and physicochemical characteristics of the studied NMs. Most of these materials were already characterized during the NanoREG2 project. Thus, for our analyses, we have employed characteristics delivered in NanoREG2.

Table 2
Categorization scheme for cytotoxicity of the nanomaterials.

Sum score points	Categorization	Category number
0-1	Non-toxic	1
2-5	Slightly toxic	2
6-9	Toxic	3

In addition to the experimentally measured toxicological characteristics, we also calculated the following electronic structure properties (Table 4 and Table S2): vertical ionization potential (IP) and electron affinity (EA) as well as IP based on Koopmans' theorem (IP'). The highest occupied (HOMO) and the lowest unoccupied (LUMO) molecular orbital energy as well as their difference (H-L) were also obtained. The latter approximates the nanomaterials' band gap. Finally, the redox potential (E) for the adiabatic $Np \rightarrow Np^+ + e^-$ process was utilized to quantify electron release ability by the nanoparticle *Np*. We applied the MP2/Def2TZVPP level of theory as implemented in Gaussian 2016-C.01 package [37]. The minimal "nanoparticle" model consists of a single TiO_2, ZnO, SiO_2 or Ag molecule embedded in water solvent as approximated by the default polarizable continuum model (PCM) [38] in a Gaussian suite of programs.

The analyses were performed with 2D HCA unsupervised machine learning technique based on connecting similarities between the objects in the space of physicochemical characteristics mapped on the endpoint values [14]. Euclidean distance was used as a measure of similarity, whereas Ward's method was used for clustering.

In the case of genotoxicity (SB) and oxidative stress (indicated by oxidatively damaged DNA), a more sophisticated methodology, the supervised partial least squares method (PLS), was employed [39]. The PLS method is a supervised machine learning method, which allows the description of linear relationships between dependent (Y) and independent (X) variables. The method assumes a transformation of the original variables (similarly to the principal component analysis) and creates a set of so-called 'latent vectors'. These new latent variables are a linear combination of the primary variables and are obtained by maximizing the covariance between the X and Y sets. In both cases of presented analyses, two latent vectors were chosen to graphically represent the relationships between nanoforms' physicochemical characteristics and exhibited outcomes.

Statistics

Statistical differences between the treatment groups in the cytotoxicity and genotoxicity assays were calculated by one-way analysis of variance (ANOVA) followed by Dunnett´s post-test to test for differences between NMs concentrations and negative control. Calculations of half maximal effective concentration (EC_{50}) values were performed by non-linear regression analysis using the four parameters Hill-equation. The difference in levels of DNA damage may often be small between treatment groups. A correlation analysis of the genotoxic effects of the NMs as a function of exposure concentration and effect (Spearman *r*) was performed. A significant correlation between concentration and effect was regarded as a significant concentration response relationship. A correlation analysis appears, however, to be sensitive to influence from deviating numbers [40]. To reduce skewness of the data, the correlation

Table 1
Scoring scheme for cytotoxicity of nanomaterials (NanoREG2 Deliverable 1.7 [13] and eNanoMapper data base (https://search.data.enanomapper.net/projects/nanoreg2/).

	Toxicity reaches			EC50[a]		
Toxicity level	20 %	50 %	80 %	< 100 μg/ml	< 60 μg/ml	< 20 μg/ml
Score Points	+ 1	+ 1	+ 1	+ 2	+ 2	+ 2

[a] EC_{50}: Concentration that gives half of the maximal response.

Table 3
Categorization scheme for genotoxicity of nanomaterials.

Categories	Criteria	Category number
Negative	Background level of damage, none of the criteria for positive are met. No significant effect	1
Equivocal	Significant linear trend OR one concentration significantly different from control	2
Positive	Significant linear trend AND at least one concentration significantly different from control; or at least two concentrations significantly higher from control	3

Table 4
Descriptors and physicochemical properties used in two-way hierarchical cluster analysis (2D HCA) (http://www.enanomapper.net).

Descriptors and physicochemical properties of studied NMs	
TEM SIZE	Stock TEM size of NPs [nm]
SHAPE	Shape of nanoparticles expressed with binary classification (1-spherical, 2-rod)
COATING PRESENCE	Intentional or unintentional presence of chemical identities on the NMs surface, expressed with binary classification (0-NMs without coating, 1-NMs with coating)
NTA Average MODE SIZE (DMEM, 0 hours)	Mode or mean average size [nm] in cell culture media DMEM at time point 0 hours
NTA Average MODE SIZE (STOCK, 0 hours)	Mode or mean average size [nm] in stock solution at time point 0 hours
SIZE INCREASE (Average MODE)	Property defining the difference between stock size [nm] on NPs in powder form (TEM measurement) and the size of NPs in the DMEM medium (NTA measurement).
HOMO	Highest occupied molecular orbital energy [a.u.]
LUMO	Lowest unoccupied molecular orbital energy [a.u.]
EA	Vertical electron affinity [eV]
IP	Vertical ionization potential [eV]
IP'	Vertical ionization potential from Koopmans' theorem [eV]
H-L	Band gap energy [eV]

analysis was therefore performed on log-transformed numbers (both concentration and effect). Statistics and regression analyses were computed in GraphPad Prism 9. Calculations were performed in Excel 2013.

Results

Size and size distribution of the NMs in dispersion

Size and size distribution of the NMs were measured by NTA in stock dispersion at time 0 h and in cell culture medium at times 0, 3 and 24 h (Fig. S1). The size of most of the NMs was found to be stable in cell culture medium DMEM and comparable with the stock dispersion. Aggregation was seen in medium compared with stock dispersion for SiO_2 NMs (NM-200 and NM-203) and for TiO_2 NMs (NM-101) at 3 h. A smaller size was measured in cell culture medium compared with stock at all time points for TiO_2 NM-104 but only at time 0 h for ZnO NM-110 and time 24 h for ZnO NM-112 (Fig. S1).

Cytotoxicity of the NMs

AlamarBlue assay

Cytotoxicity, which was measured as fluorescence intensity based on metabolic activity, was detected in A549 cells after exposure to two ZnO NMs NM-110 and NM-111, and the two Ag NMs NM-300K and NM-302 (Fig. 1). The EC_{50} values for these particles were calculated and are shown in Table 5. We have performed a ranking based on the values of EC_{50}. After 3 h, the cytotoxicity ranking from the less cytotoxic to the more toxic was found to be NM-110 < NM-111 < NM-112 < NM-113 < NM-302 < NM-300K and after 24 h NM-302 < NM-112 < NM-300K < NM-110 < NM-111 < NM-113. A slight increase in metabolic activity was seen for TiO_2 NMs NM-101 and SiO_2 NM-200 after 3 h exposure and after 24 h for the SiO_2 NM-201, NM-202 and NM-204 (Fig. S2). The statistical analysis and the toxicity scoring are shown in Tables S3&S4. According to our scoring system approach and the statistical analysis (Tables S3&S4), NM-112 and NM-113, NM-300K and NM-302 were toxic (Category 3), while NM-110 and NM-111 were scored slightly toxic (category 2) after 3 h exposure. After 24 h exposure, four NMs (NM-110, NM111, NM-113 and NM-300K) were toxic (category 3), while NM-302 and NM-112 were slightly toxic (category 2). All tested TiO_2 and SiO_2 NMs were negative (category 1) after both 3 and 24 h. The NM-300K and NM-302 solvent controls did not show cytotoxic effect (data not shown).

Colony forming efficiency assay

Cell viability was measured by colony formation (the CFE assay) and cytotoxic effects were found after exposure of A549 cells to ZnO NMs (NM-110, NM-111, NM-112, NM-113) and Ag NMs (NM-300K, NM-302) (Fig. 2). Calculated EC_{50} values for the cytotoxic NMs are shown in Table 6. None of the other NMs showed any cytotoxic effect in the CFE assay, except for the highest concentration of NM-202 (Fig. S3). There was also a general trend for the TiO_2 NMs to induce a concentration-dependent increase in number of colonies formed (Fig. S3). The NM-300K and NM-302 solvent controls did not show any cytotoxic effect (data not shown). According to our scoring system approach and the statistical analysis (Table S5), all tested ZnO NMs and both Ag NMs were scored toxic (category 3) while the other particles TiO_2 and SiO_2 NMs were categorized as negative (category 1) which seems to be in accordance with the AB assay testing.

Genotoxicity of the NMs measured as strand breaks by the comet assay

The genotoxic potentials of a total of seventeen NMs were measured on A549 cells by a medium-throughput minigel version of the comet assay. DNA strand breaks (SB) were measured by tail intensity %, and only non-cytotoxic concentrations (below or equal 60 % viability) were considered for evaluation of genotoxicity to distinguish between direct DNA damage and secondary damage due to cell death. Significant increases in DNA strand breaks (SB) were measured after 3 h exposure to SiO_2 NM-200 and NM-203, ZnO NM-110 and NM-111 and Ag NM-300K. After 24 h exposure, the increase of SB was only observed for ZnO NM-110, Ag NM-300K and SiO_2 NM-200 (Fig. 3), whereas no significant increase was observed after 3 h or 24 h with the other tested NMs, including NM-302 (Fig. 3 and S4S3). Following the statistical analysis performed (Table S6 and S7) and the scoring and categorization system described above, after 3 h exposure NM-100, NM-203 and NM-300K were categorized as positive for genotoxicity (category 3), whereas five NMs were categorized equivocal (category 2), and the other nine NMs as negative

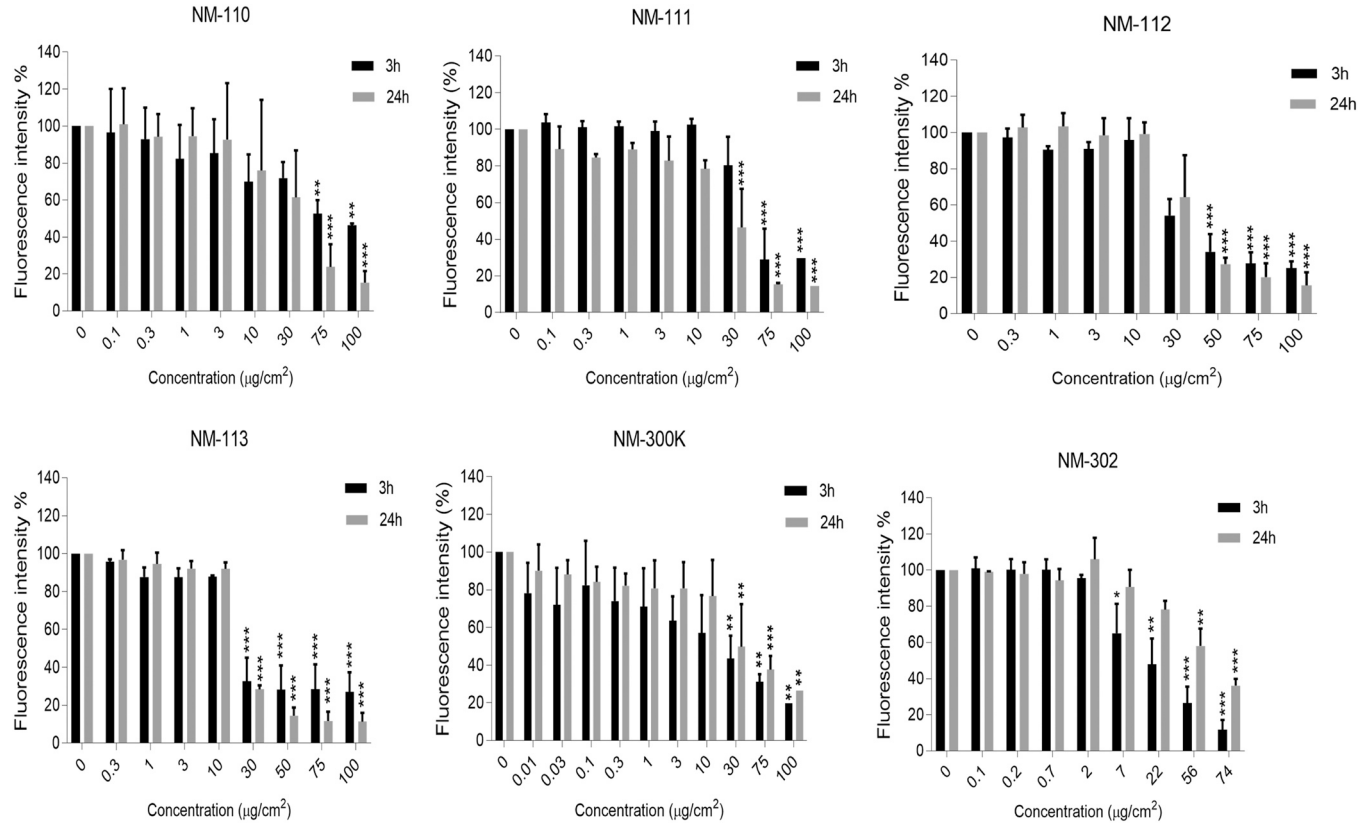

Fig. 1. Relative cell viability measured as fluorescence intensity after metabolic activation in viable cells by the AlamarBlue assay after exposure of A549 cells for 3 or 24 h to ZnO NMs (NM-110, NM-111, NM-112 and NM-113), and Ag NMs (NM-300K and NM-302). The results are shown as mean ± SD from three independent experiments. For each experiment, exposure was performed in duplicate and from each duplicate, three replicate wells were made for reading of fluorescence. Cell viability is presented relative to negative control, set to 100 %. h, hours; SD, standard deviation. Dunnett's test *p < 0,5, **p < 0.1, ***p < 0.01.

(category 1) (Fig. 5 & Table S6). After 24 h exposure, only NM-110 was categorized as positive for genotoxic effect (category 3), whereas seven NMs were categorized as equivocal (category 2), the other nine NMs were categorized as negative (category 1) (Fig. 5 & Table S7). A summary of the results obtained for the other NMs is presented in Fig. S4 and the statistical calculation for each of the NMs are shown in Tables S6 & S7 (Supplementary materials). The NM-300K and NM302 solvent controls did not induce any significant increase in SB compared to negative control (data not shown).

Induction of oxidized purines measured by the enzyme-linked version of the comet assay

For detection of oxidized DNA bases, the enzyme-linked version of the comet assay was applied. [35]. No increase in DNA base lesions was observed after 3 nor 24 h exposure. According to the statistical analysis conducted and our scoring and categorization system, all tested NMs were categorized either negative (category 1) or equivocal (category 2) at both exposure times (3 and 24 h) (Fig. 4 & S5, Table S8& S9). The NM-300K and NM-302 solvent controls did not induce any significant increase in oxidized base lesions compared to negative control (data not shown).

Toxicity categorization of the NMs

Toxicity scoring and categorization are summarized in Fig. 5, and it was performed as described above in Table 1, 2 and 3. The Ag NM-300K was ranked with the highest toxicity, whereas the TiO_2 NM-105 and the SiO_2 NM-201 were ranked as the ones with the lowest toxic potential. To present a single categorization result among biological responses for genotoxicity (SB), cytotoxicity and oxidative stress (indicated by oxidatively damaged DNA), we used the so-called "worst-case approach", in which the worst-case scenario of a particular adverse effects is assumed. Of all the effects measured for a given nanoform, the categorization value corresponding to the highest toxicity is ultimately considered (Fig. 5). For visualization of

Table 5
Calculated EC_{50} values (mean ± SEM) for the cytotoxic effects of the ZnO NMs (NM-110, NM-112 and NM-113) and Ag NMs (NM-300K and NM-302) measured by the AlamarBlue assay after exposure of A549 cells for 3 or 24 h. The results are mean values calculated from three independent experiments and concentrations given as both µg/cm² and µg/ml + /- SEM. SEM, standard error of mean; h, hours.

Nanomaterials (NMs)		3 h		24 h	
		EC_{50} (µg/cm²)	EC_{50} (µg/ml)	EC_{50} (µg/cm²)	EC_{50} (µg/ml)
ZnO	**NM-110**	104 ± 47	166 ± 76	33 ± 6.9	53 ± 11
	NM-111	54 ± 3.7	87 ± 6.0	23 ± 3.9	37 ± 6.2
	NM-112	37 ± 2.9	57 ± 4.7	38 ± 2.6	60 ± 4.1
	NM-113	26 ± 3.5	41 ± 5.6	22 ± 1.4	36 ± 2.2
Ag	**NM-300K**	12 ± 6.9	19 ± 11	37 ± 15	59 ± 43
	NM-302	14.7 ± 10.9	23.6 ± 17.4	57.9 ± 4.9	92.7 ± 7.8

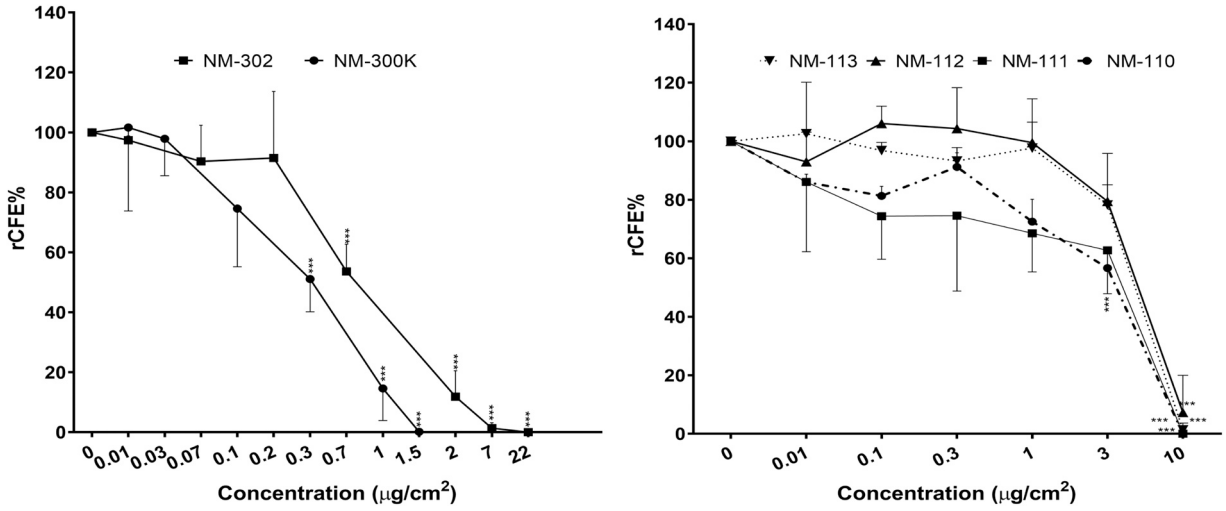

Fig. 2. Cell viability measured as relative colony forming efficiency (rCFE) in A549 cells exposed to Ag NMs NM-300K and NM-302 (left) and ZnO NMs NM-110, NM111, NM-112 and NM-113 (right) calculated relative to negative control set to 100 %. The results are shown as mean ± SD from three independent experiments with 6 replicate wells for each treatment group within each experiment. SD, standard deviation. Dunnett's test ***p < 0.01.

Table 6
Calculated EC_{50} values (mean ± SEM) for the cytotoxic effects of the ZnO-NMs (NM-110, NM-111, NM-112 NM-113), Ag NMs (NM-300K, NM-302) and SiO_2 NM-202 measured by the colony forming efficiency (CFE) assay after exposure of A549 cells. The results are calculated from 2–3 independent experiments and concentrations shown as both μg/cm² and μg/ml. SEM, standard error of mean. EC_{50}, half maximal effective concentration.

Nanomaterials (NMs)		EC_{50} (μg/cm²)	EC_{50} (μg/ml)
ZnO	**NM-110**	1.7 ± 0.4	8.4 ± 1.8
	NM-111	1.9 ± 0.8	9.1 ± 3.8
	NM-112	4.6 ± 0.5	22.0 ± 2.3
	NM-113	4.0 ± 0.5	19.0 ± 2.4
SiO_2	**NM-202**	~95	~360
Ag	**NM-300K**	0.3 ± 0.04	1.3 ± 0.2
	NM-302	1.01 ± 0.4	4.87 ± 1.92

the effect, we have followed the convention used for this type of analysis [41].

In silico identification of descriptors for cyto- and genotoxicity by chemometric analysis

The chemometric analysis with the use of 2D-HCA identified distinct descriptors for cyto- and genotoxicity for a grouping approach for hazard identification of NMs. In the case of cytotoxicity, the properties that identified highly toxic nanoforms were mainly related to their calculated quantum mechanical properties, namely: electron affinity (EA), ionization potential (IP, IP'), electronic energy (E), energy of the highest occupied molecular orbital (HOMO), energy of the lowest unoccupied molecular orbital (LUMO) and band gap energy (H-L) (Fig. 7). One NM, NM-202, exhibited slight cytotoxicity; however, no clear relationships with its properties were

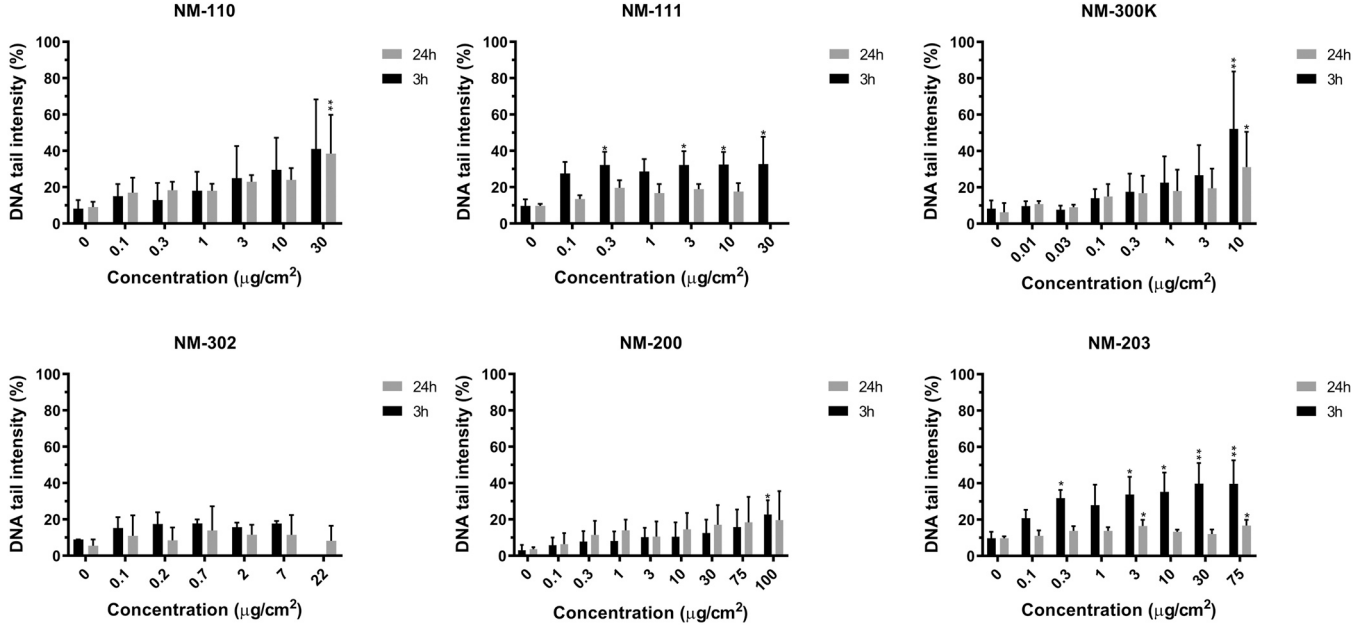

Fig. 3. DNA damage by strand breaks measured by the comet assay as tail intensity induced by ZnO NMs NM-110 and NM-111, Ag NMs NM-300K and NM-302 and SiO_2 NM-200 and NM-203, in A549 cells after 3 h and 24 h. Three independent experiments were performed with duplicate wells for each exposure. The results are shown as mean of the median of duplicate wells from each of the three experiments ± SD. h, hours; SD, standard deviation. Dunnett's test *p < 0.5, **p < 0.1, ***p < 0.01.

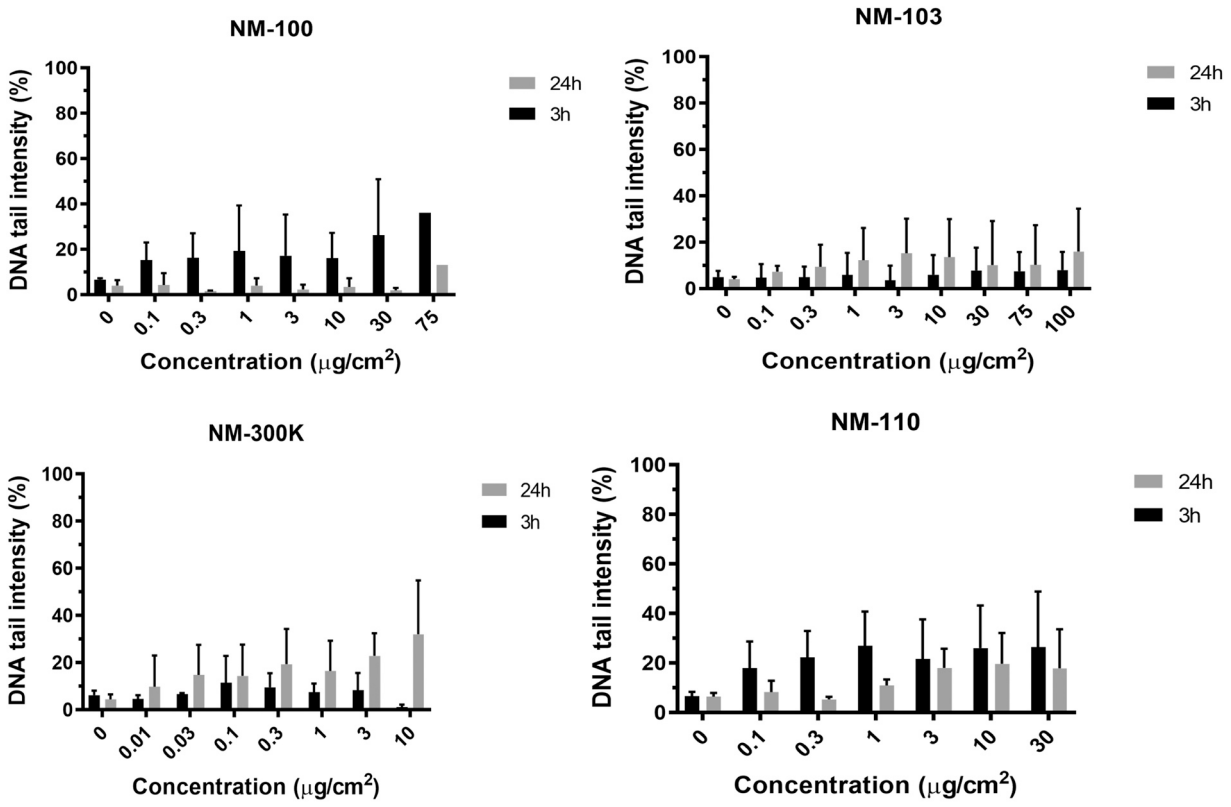

Fig. 4. Induction of oxidized DNA bases measured as tail intensity by the enzyme-linked version of the comet assay with formamidopyrimidine glycosylase (Fpg) after exposure of A549 cells to TiO_2 NMs NM-100 and NM-103, Ag NM NM-300K and ZnO NM NM-110 for 3 or 24 h. Three independent experiments were performed with duplicate wells for each exposure. The results are shown as mean of the median of duplicate wells from each of the three experiments ± SD. h, hours; SD, standard deviation.

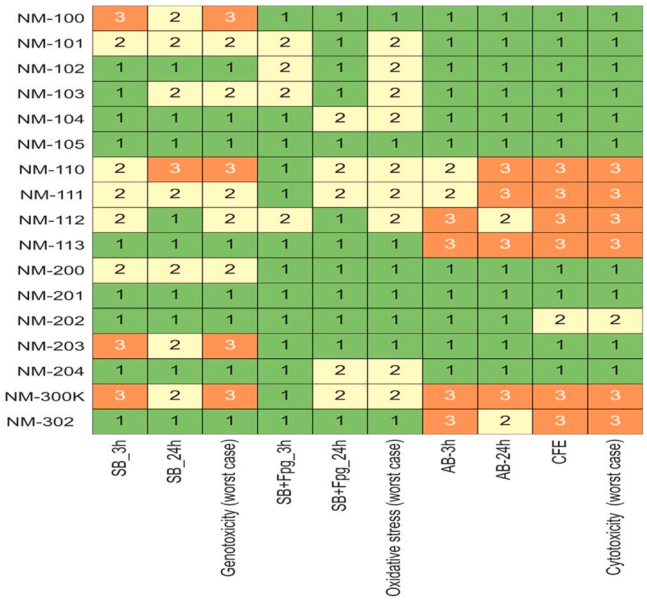

Fig. 5. Overview of the categorization of the tested nanomaterials (NMs) for genotoxicity by the enzyme-linked version of the comet assay for both DNA strand breaks (SB) and oxidized lesions (SB+Fpg) after 3 or 24 h, cytotoxicity by the AlamarBlue assay after 3 or 24 h and the colony forming efficiency assays. The corresponding worst-case scenarios are also presented. ; AB, Alamarblue; CFE, colony forming efficiency. Categories for cytotoxicity; 1: non-toxic, 2 = slightly toxic, 3 = toxic. Categories for genotoxicity: 1 = negative, 2 = equivocal, 3 = positive. NA= not available data; h, hours, NMs; nanomaterials, Fpg; formamidopyrimidine.

visible. It can also be observed that the silver NMs, NM-300K and NM-302, exhibited the lowest values of band gap energy and ionization potential, as well as the highest HOMO and electronic energies. (Fig. 6).

For genotoxicity, the 2D-HCA analysis did not reveal a clear correlation between the NMs' properties and exhibited effects defined by the worst-case approach. Thus, the PLS method was additionally applied (Fig. 7, Table S2). This analysis allowed grouping of the NMs in the multidimensional space of physicochemical properties, descriptors and observed activity (genotoxicity scoring). By implementing the PLS approach, we revealed properties which at least differentiated groups of positive/equivocal from negative NMs based on the Latent Vector 1 (LV1, x-axis) where the band gap (H-L) and HOMO energies as well as the ionization potential (IP') were the most influential, whereas for the LV2 (y-axis), the TEM size was the most influential. One NM with a high genotoxicity (SB) (NM-203) did not sit within this group.

Similarly, the 2D-HCA analysis did not show any clear relationship between the NMs' characteristics and induced oxidative stress (indicated by oxidatively damaged DNA), and so the PLS was applied (Fig. 8, Table S2).

The analysis revealed a separate group of five NMs (NM-101, NM-103, NM-104, NM-110, NM-111) which exhibited a similar, 'equivocal' category of oxidative stress. All these NMs were identified as having deliberate or unintentional presence of organic/inorganic chemical identities on their surface (coating presence property).

Discussion

Human hazard identification and characterization should be supported by identification of descriptors for prediction of toxicity. This is essential for risk assessment to cope with the rapid development of new NMs, the SbD approach and the 3Rs to reduce, refine and replace animal experiments. A highly challenging aspect of NMs

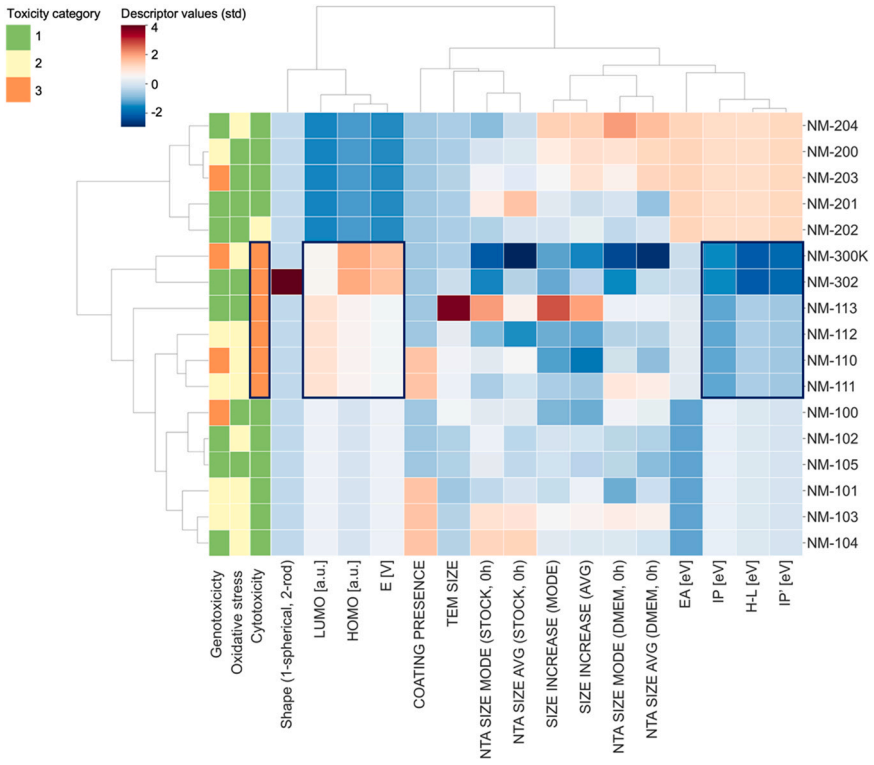

Fig. 6. 2D Hierarchical Clustering Analysis of selected nanomaterials in the space of descriptors. The first three columns depict the assumed worst-case genotoxicity, oxidative stress (indicated by oxidatively damaged DNA) and cytotoxicity of NMs. The remaining matrix cells reflect the values of individual properties corresponding to NMs. White or close to white cells correspond to values close to the overall average of the descriptor. Values that are very high (+3 standard deviations from mean) are marked as dark red, whereas very low values (−3 standard deviations from mean) are marked as dark blue. The more a property for a given NM differs from the average, the more saturated will be its cell color. Categories for cytotoxicity; 1: non-toxic, 2 = slightly toxic, 3 = toxic. NMs, nanomaterials. NTA, nanoparticle tracking analysis; LUMO, lowest unoccupied molecular orbital; HOMO, highest occupied molecular orbital; E, electronic energy; H-L, band gap energy; EA, electron affinity; IP, ionization potential; h, hours; AVG, average.

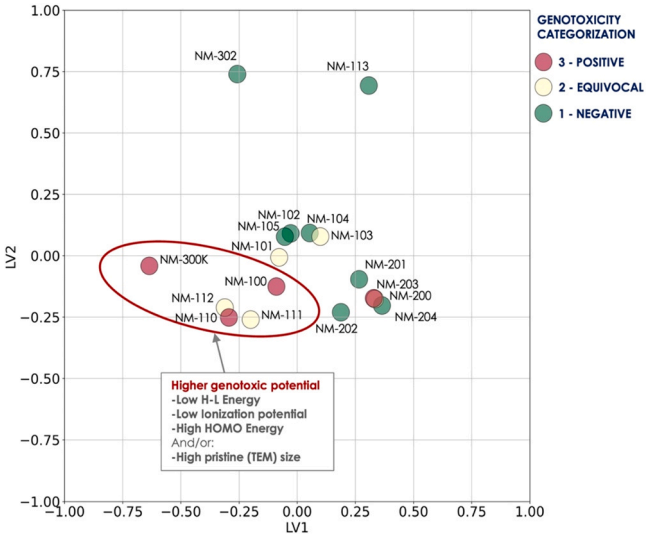

Fig. 7. Scatter plot for NMs' genotoxicity (strand breaks) by means of partial least method (PLS) analysis. TEM, transmission electron microscopy; HOMO, highest occupied molecular orbital; H-L, gap band, LV1 and LV2 Latent Vector 1 and 2.

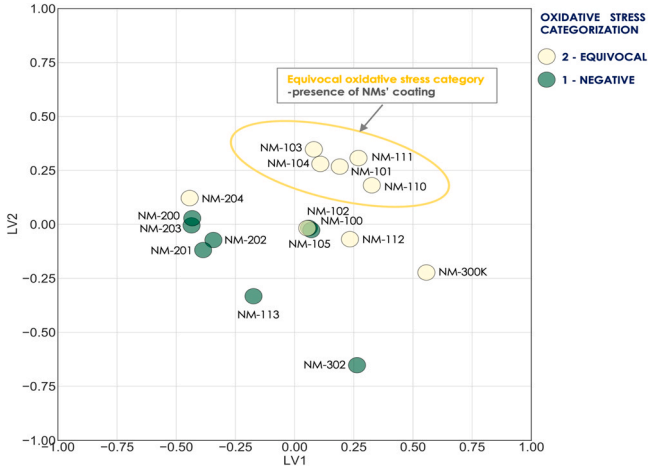

Fig. 8. Scatter plot for nanomaterial (NM)-induced oxidative stress (oxidatively damaged DNA) by means of partial least squares method (PLS) analysis. LV1 and LV2 Latent Vector 1 and 2.

is the implication of physicochemical properties for their toxicity, such as size, charge, agglomeration and surface coating, as well as binding of proteins and protein corona [42]. We report here a concerted effort to characterize hazard and categorize cytotoxic and genotoxic potential of several groups of NMs namely TiO_2, SiO_2, ZnO and Ag with distinct properties, to help identify descriptors for toxicity by chemoinformatic analysis.

In this study, six TiO_2 NMs, five SiO_2 NMs, two Ag-NMs and four ZnO NMs, all with different physicochemical properties, were tested for cytotoxicity and genotoxicity in human lung epithelial cells A549. In our work, the cytotoxicity testing using the AB and CFE assays showed that both Ag NMs and the four ZnO NMs tested were cytotoxic. The chemoinformatic analyses, including 2D-HCA and PLS, revealed relationships between the NMs' physicochemical properties and their cytotoxicity. The cytotoxicity was strongly correlated with parameters describing the electron structures of NMs' main components i.e. electron affinity (EA), ionization potential (IP, IP')

and band gap energy (H-L). These descriptors are linked to characteristics such as high solubility and reactivity of the NM and could reflect release of ions from the NMs surface and their adverse affection on the cellular integrity, homeostasis, and viability. Thus, the most toxic NMs tested were the soluble ones, Ag and ZnO, which agrees with the work of García-Rodríguez *et al*. using the same materials [43], whereas the SiO_2 NMs and TiO_2-NMs were found to be non-cytotoxic due to being poorly soluble or insoluble. As shown by Kononenko *et al*. [44], NMs that are known to be either slightly soluble or insoluble in aqueous media (such as SiO_2) were only moderately cytotoxic to A549 cells [44]. Similar results on both A549 cells and macrophage-like THP-1 cells were reported by Jeong *et al.* [45], who showed that fast dissolving NPs do not always have similar toxic potentials compared to their constituent metal chlorides, and that this may be due to the differences in their cellular uptake [45]. Once endocytosed, poorly soluble or insoluble nanoparticles could either accumulate in the acid endo-lysosomal organelles or leave the cell by exocytosis [46].

Based on the categorization approach for the genotoxic potential and the worst-case scenario applied, we defined one TiO_2 (NM-100) out of six tested, one ZnO (NM-110) out of four tested, one SiO_2 out of five tested and one Ag (NM-300K) out of two tested, to be clearly genotoxic causing single SB. While the other NMs were categorized either as negative or equivocal. Further testing is needed to be able to conclude on genotoxic potential specifically of the last group (NMs categorized as equivocal). The applied 2D-HCA analysis did not reveal a clear correlation between NM properties and exhibited genotoxic effect defined by the worst-case approach. The PLS analysis, however, indicated that similar descriptors that influenced cytotoxicity of some NMs also had implications for their genotoxicity, such as low band gap energy and ionization potential and high HOMO energy (Fig. 8).

The TiO_2 NMs (from JRC), known as titanium (IV), occurs in nature as the rutile and anatase minerals [47] having distinct electrical and optical properties, which may have implications for their toxicity. The anatase crystal form is the less thermodynamically stable, and generally expected to be more cytotoxic than rutile or anatase/rutile mixture because of its strong photocatalytic properties [48–50]. Anatase may spontaneously generate reactive oxygen species (ROS), and ROS may also arise after exposure to light or due to sufficient energy available in test medium to generate electron hole at the NM surface [51]. In some studies, anatase TiO_2 NM was more toxic than rutile TiO_2 NM, which agrees with the perception of the rutile forms as chemically inert and anatase forms as more reactive. This is consistent with our findings, as the only TiO_2 NM found to be genotoxic in this study was the anatase TiO_2 NM-100. This is also in agreement with the findings by Di Bucchianico *et al*., [52] showing genotoxic effects of NM-100 on Beas2B cells and less pronounced effect of the TiO_2 NM-101 and NM-103. However, in other studies, the contrary is seen, with rutile TiO_2 NMs showing higher toxicity than anatase TiO_2 NMs [53]. So, basically, crystallinity seems to have an impact on the genotoxic potential of TiO_2 as it seems that both anatase and rutile can form ROS when they interact with the cellular components [54].

In addition to their inherent physicochemical properties and behavior in the exposure medium, it is also imperative that the type of cell used is considered when comparing rutile and anatase, as cells may have different anatase and rutile uptake capacities, which would affect the toxicity of these NMs [55]. In the work of Andersson *et al*. the cellular uptake and distribution of five types of well-characterized anatase and rutile TiO_2 NMs were investigated in A549 lung epithelial cells. NMs uptake was found to be kinetically activated and strongly dependent on the hard agglomeration size and not the primary particle size [56]. In addition, it was also observed that ZnO nano-forms are more cytotoxic than the ZnO micro-form, which also means that size is an important factor for determining cytotoxicity [44]. It has also been shown that larger nanoparticles or agglomerated particles dissolve more slowly than small sized particles [57]. This is mainly due to the endocytosis phenomenon which is size and surface area of the NMs dependent [46,58]. Smaller aggregates were more prone to uptake and reflect the ability of nanoparticles to interact with DNA, either indirectly, such as impairing DNA repair, or even by penetrating into the nucleus and exhibiting direct interaction with the DNA. Andersson *et al.* also showed that uptake of the TiO_2 materials was positively correlated to induction of oxidative stress and inflammation in the cells [56]. It is clear that TiO_2 NMs have potential toxicity on a variety of cell types and tissues. Moreover, they tend to have different cellular distribution and ability to damage various organelles or exhibit different interaction activity with biomolecules [55]. The International Agency for Research on Cancer (IARC) concluded that there is sufficient evidence of carcinogenicity in experimental animals, but inadequate evidence of carcinogenicity in humans, with an overall evaluation of TiO_2 NM as “possibly carcinogenic to humans” (Group 2B) [59]. Recently, EFSA evaluated TiO_2 E171 (nano and microparticles) in food and considered them not to be safe due to their potential genotoxicity [60].

Nanosized silica is among the mostly used NMs, usually as amorphous forms produced by precipitation (NM-200, NM-201) or by thermal synthesis (NM-202, NM-203). In our study we noticed that two silica NMs out of five, NM-200 and NM-203, were categorized as equivocal and positive for genotoxicity respectively. In previous studies, it has been observed that most of the tested silica NMs have been found not to be genotoxic [61–64]. In a study by Lu *et al*. (2015), the tested SiO_2 NMs induced neither cellular oxidative stress nor DNA damage by the comet assay [65]. The silica materials used in our study differ from each other with respect to physical characteristics such as shape, specific surface area (160–230 m^2/g), and primary particle size (8–20 nm). However, we could not identify particular properties of NM-203 that could explain its genotoxicity. This may be due to insufficient material characterization which did not allow linking of structural diversity to the observed genotoxicity of silica NMs. In this study, only descriptors that were fully measured within NANoREG and NanoREG2 projects were included in the chemometrics analysis.

Crystalline silica is classified as a carcinogen, but the genotoxicity of both crystalline and amorphous silica particles remains unclear. Amorphous silica is regarded as less toxic than crystalline silica, partly due to a higher clearance rate leading to less chronic inflammations [66]. Recent studies have indicated that both crystalline and amorphous silica particles may be non-genotoxic carcinogens as shown by Bhas 42 cell transformation assays [63,64]. In a study by Skuland *et al.* (2020), both crystalline and amorphous silica particles induced release of pro-inflammatory cytokines/adhesion molecules in an advanced 3D-triculture model of the epithelial A549 cells, endothelial EA.hy926 cells and THP-1 macrophages [67]. The SiO_2 NMs have shown effects on viability of the human pulmonary alveolar epithelial cells (HPAEpiC) by increasing the expression levels of two endoplasmic reticulum (ER) stress markers that can be attributed to inflammatory responses [68].

A crucial component of the toxicity of Ag and ZnO NMs is attributed to their high solubility rate and it is postulated that increased solubility increases toxicity [69]. There is still a discussion as to whether it is the particles themselves or released ions that exert the prime effects of soluble NMs. Probably it is a combination since the solubility of metal NMs depends on several factors, such as size, shape, coating and the pH of the surrounding micro-environment. Our 2D HCA revealed also a new parameter which might explain the toxic effect of these materials; both NM-300K and NM-302 exhibited the lowest values of band gap energy and ionization potential, as well as the highest HOMO and electronic energies.

Previous studies using the same Ag NMs have shown their genotoxic effects [70], whereas genotoxic studies of ZnO NMs have been

less conclusive [71]. In this work the spherical Ag NMs were, on a mass base, more toxic than the fibrous Ag materials, which may be explained by their ability to penetrate the cells either faster or better than fibrous Ag. When inside the cells, the Ag NMs may release more ions due to the acidic micro-environment in the phagocytes, leading to more effects. This was shown in a study by Bobyk *et al.* (2021), in which A549 cells were exposed to NM-300K and to a larger spherical PVP-coated Ag NM. The Ag NMs showed differential transformation and toxicity due to their size, coating and dissolution potential. NM-300K was the most toxic with higher intracellular accumulation and dissolution [72]. The same mechanisms may also be valid for the soluble ZnO NMs as it has also been reported that internalized ZnO NMs in acidic endosomes/lysosomes completely dissolves and Zn^{2+} ions released from the ZnO NMs results in cellular toxicity [73–75]. Based on presented analysis (Fig. 7), we may conclude that with the decreasing values of H-L and IP energies and increasing values of HOMO energy, the genotoxicity will also increase. Thus, for instance, the highest genotoxic potential was observed for Ag and ZnO NMs. Additionally, in some cases the NMs with high genotoxic potential showed relatively higher pristine size (TEM), in the range of 50–120 nm.

The level of oxidized base lesions (oxidized purines), which is an important biomarker for oxidative stress, has also been evaluated. Oxidative stress occurs when there is imbalance between ROS formation and antioxidant capacity, and it is one of the main mechanisms of action leading to several adverse outcomes following the exposure to NMs [76]. ROS can be formed via transition metal ions released from the NM surface, by other chemicals on the particle surface, or as a consequence of the interaction between particles and cellular components, such as mitochondria [76,77]. Interestingly, the PLS analysis of the data obtained from the Fpg-modified comet assay showed that coated NMs had greater potential to induce oxidative stress than uncoated NMs. This observation was quite surprising, since the literature provides information that the presence of the coating will minimize the production of ROS by covering the active NM surface [78,79]. On other hand, there is also evidence that the coating may influence the behavior of NMs in medium, can increase ROS production and may itself release toxic materials. The presence of transition metals on the surface of the NM may lead to generation of ROS and it has been shown that surface coatings can be degraded, for instance due to etching in acidic or alkaline conditions [80], potentially revealing the more toxic metallic core [81]. It can be concluded that the presence of a surface coating may cause higher oxidative stress; it should also be noted, however, that the 'coating presence' property does not provide specific information on the chemical composition of the coating itself. Within the second group identified by PLS, analysis of data from the Fpg-modified comet assay, most of the uncoated NMs exhibited a 'negative' effect. Exceptionally, four NMs (NM-102, NM-112, NM-204, NM-300K), despite not having a coating, induced oxidatively damaged DNA. In turn, our results indicate that some coatings can induce a higher surface activity of the NM. The NMs we tested in this work have diverse chemical compositions (TiO_2, ZnO, SiO_2, Ag), and despite their close similarity to the 'negative' NMs (within analyzed properties), the reason for the higher potential of some particles to induce oxidative stress may be related to properties that were not included in the characterization. Due to the limitation in literature regarding available data on the use of coating, and also due to the wide nature of coating available, we believe more detailed characterization of the NMs is required to obtain more specific analyses that would confirm observed relationships and extend their applicability.

We would like to stress that the work presented here doesn't introduce grouping for regulatory applications. For our analysis we included four chemically different groups of NMs to identify factors that can drive toxicity and to support mechanistic hypotheses. By using different experimental and *in silico* methods and different groups of NMs, the work can serve as base for developing of grouping hypotheses that can be later tested more thoroughly.

Conclusion

The presented work marks an important step within human hazard and safety assessment of NMs, by applying *in silico* modeling to identify NMs physicochemical descriptors to predict human hazard and reduce risk of adverse health effects. We applied the NanoREG2 categorization approach for our cytotoxicity and genotoxicity data after testing of a range of NMs, and we were able to identify distinct descriptors for prediction of toxicity of NMs to support development of grouping hypotheses that can be later tested more thoroughly. Following our PLS analysis we identified descriptors such as band gap (H-L) and HOMO energies as well as the ionization potential (IP') linked to genotoxic potential of NMs. Further, coated particles had greater potential to induce oxidatively damaged DNA than uncoated, and the soluble NMs were the most cytotoxic ones. The use of an integrated approach combining experimental and *in silico* analysis facilitated relationship between NMs physicochemical descriptors and the observed effect. Development and use of machine learning-based analyses has the potential to be a powerful tool in the *in silico* risk assessment of NMs and will support the safer-by design approach.

CRediT authorship contribution statement

Naouale El Yamani: Conceptualization, Methodology, Data curation, Formal analysis, Writing- Reviewing and Editing. **Espen Mariussen**: Conceptualization, Methodology, Data curation, Formal analysis, Writing and reviewing. **Maciej Gromelski**: Methodology, Data curation, Formal analysis, Writing and Reviewing. **Ewelina Wyrzykowska**: Methodology, Data curation, Formal analysis, Writing - review & editing. **Dawid Grabarek**: Methodology and Data curation. **Tomasz Puzyn:** Conceptualization and Methodology. **Speranta Tanasescu**: Conceptualization. **Maria Dusinska**: Funding acquisition, Methodology, Project administration, Resources, Validation, Formal Analysis, Supervision, Conceptualization, Writing- Reviewing and Editing. **Elise Rundén-Pran:** Project administration, Resources, Methodology, Formal Analysis, Supervision, Conceptualization, Writing- Reviewing and Editing.

Data availability

Data will be made available on request.

Declaration of Competing Interest

The authors declare that they have no known competing financial interests or personal relationships that could have appeared to influence the work reported in this paper.

Acknowledgements

This work was supported by the EC FP7 NANoREG [grant agreement NMP4-LA-2013–310584, 2013]; the Research Council of Norway, project NorNANoREG [239199/O70, 2015]; the European Union's Horizon 2020 research and innovation program projects NanoREG2 [grant agreement 646221, 2015]; the European Union's Horizon 2020 research and innovation program projects RiskGONE [grant agreement 814425, 2019]; the European Union's Horizon 2020 research and innovation program projects NanosolveIT [grant agreement 814572, 2019]; VISION [grant agreement 857381, 2019] and TWINALT [grant agreement 952404, 2020].

Supporting Information

Supporting Information is available from the Wiley Online Library or from the author.

Appendix A. Supporting information

Supplementary data associated with this article can be found in the online version at doi:10.1016/j.nantod.2022.101581.

References

[1] T.V. Teunenbroek, J. Baker, A. Dijkzeul, Part. Fibre Toxicol. 14 (2017) 54.
[2] V. Stone, H.J. Johnston, D. Balharry, J.M. Gernand, M. Gulumian, Risk Anal.: Off. Publ. Soc. Risk Anal. 36 (2016) 1538–1550.
[3] A.R. Collins, B. Annangi, L. Rubio, R. Marcos, M. Dorn, C. Merker, I. Estrela-Lopis, M.R. Cimpan, M. Ibrahim, E. Cimpan, M. Ostermann, A. Sauter, N.E. Yamani, S. Shaposhnikov, S. Chevillard, V. Paget, R. Grall, J. Delic, F.G. de-Cerio, B. Suarez-Merino, V. Fessard, K.N. Hogeveen, L.M. Fjellsbø, E.R. Pran, T. Brzicova, J. Topinka, M.J. Silva, P.E. Leite, A.R. Ribeiro, J.M. Granjeiro, R. Grafström, A. Prina-Mello, M. Dusinska, Wiley interdisciplinary reviews, Nanomed. Nanobiotechnol. 9 (2017).
[4] J.A. Shatkin, K.J. Ong, C. Beaudrie, A.J. Clippinger, C.O. Hendren, L.T. Haber, M. Hill, P. Holden, A.J. Kennedy, B. Kim, M. MacDonell, C.M. Powers, M. Sharma, L. Sheremeta, V. Stone, Y. Sultan, A. Turley, R.H. White, Risk Anal.: Off. Publ. Soc. Risk Anal. 36 (2016) 1520–1537.
[5] V. Stone, S. Gottardo, E.A.J. Bleeker, H. Braakhuis, S. Dekkers, T. Fernandes, A. Haase, N. Hunt, D. Hristozov, P. Jantunen, N. Jeliazkova, H. Johnston, L. Lamon, F. Murphy, K. Rasmussen, H. Rauscher, A.S. Jiménez, C. Svendsen, D. Spurgeon, S. Vázquez-Campos, W. Wohlleben, A.G. Oomen, Nano Today 35 (2020) 100941.
[6] REACH, 2018. From ⟨https://eur-lex.europa.eu/legal-content/EN/TXT/PDF/?uri=CELEX:32018R1881&from=EN⟩.
[7] ECHA, 2017. Appendix R.6–1: Recommendations for nanomaterials applicable to the Guidance on QSARs and Grouping of Chemicals. From ⟨https://echa.europa.eu/documents/10162/13564/appendix_r6–1_nano_draft_for_committees_en.pdf/cb821783-f534–38cd-0772–87192799b958⟩.
[8] ECHA, ECHA2019. From ⟨https://echa.europa.eu/documents/10162/7312408/FINAL_MB_06_2020_Annual_Report_2019_incl_CAAR_and_MB_assessment_MB57.pdf/8b80af23–0a1c-3676–75d8-fa6d0d1dd02c⟩.
[9] ECHA, 2017. Read-Across Assessment Framework (RAAF). https://echa.europa.eu/documents/10162/13628/raaf_en.pdf/614e5d61–891d-4154–8a47–87efebd1851a.
[10] J.H. Arts, M.A. Irfan, A.M. Keene, R. Kreiling, D. Lyon, M. Maier, K. Michel, N. Neubauer, T. Petry, U.G. Sauer, D. Warheit, K. Wiench, W. Wohlleben, R. Landsiedel, Regulatory toxicology and pharmacology, Regul. Toxicol. Pharmacol. 76 (2016) 234–261.
[11] J.H. Arts, M. Hadi, M.A. Irfan, A.M. Keene, R. Kreiling, D. Lyon, M. Maier, K. Michel, T. Petry, U.G. Sauer, D. Warheit, K. Wiench, W. Wohlleben, R. Landsiedel, Regul. Toxicol. Pharmacol. 71 (2015) S1–S27.
[12] N. Jeliazkova, M.D. Apostolova, C. Andreoli, F. Barone, A. Barrick, C. Battistelli, C. Bossa, A. Botea-Petcu, A. Châtel, I. De Angelis, M. Dusinska, N. El Yamani, D. Gheorghe, A. Giusti, P. Gómez-Fernández, R. Grafström, M. Gromelski, N.R. Jacobsen, V. Jeliazkov, K.A. Jensen, N. Kochev, P. Kohonen, N. Manier, E. Mariussen, A. Mech, J.M. Navas, V. Paskaleva, A. Precupas, T. Puzyn, K. Rasmussen, P. Ritchie, I.R. Llopis, E. Rundén-Pran, R. Sandu, N. Shandilya, S. Tanasescu, A. Haase, P. Nymark, Nat. Nanotechnol. 16 (2021) 644–654.
[13] NanoREG2, 2019. Deliverable D 1.7, Report on Validated grouping approach, Version 2, 11/10/2019, ⟨https://ec.europa.eu/research/participants/documents/downloadPublic?documentIds=080166e5c834333c&appId=PPGMS⟩.
[14] F. Murtagh, P. Contreras, WIREs Data Min. Knowl. Discov. 7 (2017) e1219.
[15] A. Huk, A.R. Collins, N. El Yamani, C. Porredon, A. Azqueta, J. de Lapuente, M. Dusinska, Mutagenesis 30 (2015) 85–88.
[16] A. Huk, E. Izak-Nau, N. El Yamani, H. Uggerud, M. Vadset, B. Zasonska, A. Duschl, M. Dusinska, Part. Fibre Toxicol. 12 (2015) 25.
[17] A. Huk, E. Izak-Nau, B. Reidy, M. Boyles, A. Duschl, I. Lynch, M. Dusinska, Part. Fibre Toxicol. 11 (2014) 65.
[18] A. Precupas, D. Gheorghe, A. Botea-Petcu, A.R. Leonties, R. Sandu, V.T. Popa, E. Mariussen, E.Y. Naouale, E. Rundén-Pran, V. Dumit, Y. Xue, M.R. Cimpan, M. Dusinska, A. Haase, S. Tanasescu, Chem. Res. Toxicol. 33 (2020) 2054–2071.
[19] A. Collins, N. El Yamani, M. Dusinska, Free Radic. Biol. Med. 107 (2017) 69–76.
[20] N. El Yamani, A.R. Collins, E. Runden-Pran, L.M. Fjellsbo, S. Shaposhnikov, S. Zienolddiny, M. Dusinska, Mutagenesis 32 (2017) 117–126.
[21] K. Rasmusen, 2014. ⟨https://op.europa.eu/en/publication-detail//publication/0ca3a430-cd22–4eea-9d29-e2953b290b71/language-en/format-PDF/source-search⟩.
[22] C. Singh, 2011. from ⟨https://publications.jrc.ec.europa.eu/repository/handle/JRC64075⟩.
[23] K. Rasmusen, 2013. from ⟨https://op.europa.eu/en/publication-detail//publication/7b93921d-e0be-4d73-beae-2061981861b2/language-en/format-PDF/source-search⟩.
[24] C.L. Klein, Publications Office of the European Union, (2011).
[25] JRC, 2011. from ⟨https://publications.jrc.ec.europa.eu/repository/handle/JRC60709⟩.
[26] JRC, 2018. from ⟨https://publications.jrc.ec.europa.eu/repository/handle/JRC110379⟩.
[27] OECD, 2010. fom ⟨https://www.oecd.org/officialdocuments/publicdisplaydocumentpdf/?cote=env/jm/mono⟩⟨(2009)20/rev&doclanguage=en⟩.
[28] NANoREG, 2016. D5_06, from ⟨https://www.rivm.nl/sites/default/files/2019–01/NANoREG_D5_06_DR_Identification_and_optimization_of_the_most_suitable_in_vitro_methodology_Yo3qmgPoS9aEh1–9l2OVcA.pdf⟩.
[29] V. Filipe, A. Hawe, W. Jiskoot, Pharm. Res. 27 (2010) 796–810.
[30] NANOGENOTOX, 2012, The Generix NANOGENOTOX dispersion protocol-Standard operation Procedure (SOP) and Background Documentation. From ⟨https://www.anses.fr/en/system/files/nanogenotox_deliverable_5.pdf⟩.
[31] E. Elje, M. Hesler, E. Rundén-Pran, P. Mann, E. Mariussen, S. Wagner, M. Dusinska, Y. Kohl, Mutat. Res. 845 (2019) 403033.
[32] JRC, Joint Research Centre – Institute for Health and Consumer Protection, Publications Office of the European Union,, Luxembourg, 2014, p. 2015.
[33] J. Ponti, R. Colognato, H. Rauscher, S. Gioria, F. Broggi, F. Franchini, C. Pascual, G. Giudetti, F. Rossi, Toxicol. Lett. 197 (2010) 29–37.
[34] M. Dusinska, A.R. Collins, Mutagenesis 23 (2008) 191–205.
[35] A.R. Collins, M. Dusinská, C.M. Gedik, R. Stětina, Environ. Health Perspect. 104 (Suppl 3) (1996) 465–469.
[36] Z. Magdolenova, Y. Lorenzo, A. Collins, M. Dusinska, J. Toxicol. Environ. Health Part A 75 (2012) 800–806.
[37] C. Møller, M.S. Plesset, Phys. Rev. 46 (1934) 618–622.
[38] J. Tomasi, B. Mennucci, R. Cammi, Chem. Rev. 105 (2005) 2999–3094.
[39] W.J. Dunn III, S. Wold, U. Edlund, S. Hellberg, J. Gasteiger, Quant. Struct. -Act. Relatsh. 3 (1984) 131–137.
[40] C. Pernet, R. Wilcox, G. Rousselet, Front. Psychol. 3 (2013).
[41] N. Jeliazkova, E. Bleeker, R. Cross, A. Haase, G. Janer, W. Peijnenburg, M. Pink, H. Rauscher, C. Svendsen, G. Tsiliki, A. Zabeo, D. Hristozov, V. Stone, W. Wohlleben, NanoImpact 25 (2022) 100366.
[42] S.W. Shin, I.H. Song, S.H. Um, Nanomaterials 5 (2015) 1351–1365.
[43] A. García-Rodríguez, L. Rubio, L. Vila, N. Xamena, A. Velázquez, R. Marcos, A. Hernández, Nanomaterials 9 (2019).
[44] V. Kononenko, D.B. Warheit, D. Drobne, Nanomaterials 9 (2019) 704.
[45] J. Jeong, S.-H. Kim, S. Lee, D.-K. Lee, Y. Han, S. Jeon, W.-S. Cho, Front. Pharmacol. 9 (2018).
[46] N. Oh, J.H. Park, Int. J. Nanomed. 9 (Suppl 1) (2014) 51–63.
[47] H. Shi, R. Magaye, V. Castranova, J. Zhao, Part. Fibre Toxicol. 10 (2013) 15.
[48] C. Xue, J. Wu, F. Lan, W. Liu, X. Yang, F. Zeng, H. Xu, J. Nanosci. Nanotechnol. 10 (2010) 8500–8507.
[49] J. Wang, Y. Fan, Int. J. Mol. Sci. 15 (2014) 22258–22278.
[50] T. Luttrell, S. Halpegamage, J. Tao, A. Kramer, E. Sutter, M. Batzill, Sci. Rep. 4 (2014) 4043.
[51] C. Jin, Y. Tang, F.G. Yang, X.L. Li, S. Xu, X.Y. Fan, Y.Y. Huang, Y.J. Yang, Biol. Trace Elem. Res. 141 (2011) 3–15.
[52] S. Di Bucchianico, F. Cappellini, F. Le Bihanic, Y. Zhang, K. Dreij, H.L. Karlsson, Mutagenesis 32 (2017) 127–137.
[53] J. Sund, J. Palomäki, N. Ahonen, K. Savolainen, H. Alenius, A. Puustinen, J. Proteom. 108 (2014) 469–483.
[54] S. Charles, S. Jomini, V. Fessard, E. Bigorgne-Vizade, C. Rousselle, C. Michel, Nanotoxicology 12 (2018) 357–374.
[55] Q. Yu, H. Wang, Q. Peng, Y. Li, Z. Liu, M. Li, J. Hazard. Mater. 335 (2017) 125–134.
[56] P.O. Andersson, C. Lejon, B. Ekstrand-Hammarström, C. Akfur, L. Ahlinder, A. Bucht, L. Osterlund, Small 7 (2011) 514–523.
[57] A. Yang, J. Wu, C. Deng, T. Wang, P. Bian, Bull. Environ. Contam. Toxicol. 101 (2018) 514–520.
[58] S. Zhang, H. Gao, G. Bao, ACS Nano 9 (2015) 8655–8671.
[59] IARC, 2010. IARC Monographs on the Evaluation of Carcinogenic Risks to Humans VOLUME 93 Carbon Black, Titanium Dioxide, and Talc.
[60] EFSA, EFSA J. 19 (2021) e06585⟨https://www.efsa.europa.eu/en/efsajournal/pub/6585⟩.
[61] M. Yazdimamaghani, P.J. Moos, M.A. Dobrovolskaia, H. Ghandehari, Nanomed.: Nanotechnol. Biol. Med. 16 (2019) 106–125.
[62] P.J.A. Borm, P. Fowler, D. Kirkland, Part. Fibre Toxicol. 15 (2018) 23.
[63] C. Fontana, A. Kirsch, C. Seidel, L. Marpeaux, C. Darne, L. Gaté, A. Remy, Y. Guichard, Mutat. Res. 823 (2017) 22–27.
[64] A. Delic, E. Mariussen, E.D. Roede, A. Krivokapic, A. Erbe, M. Lindgren, M. Benelmekki, M.A. Einarsrud, ChemPlusChem 86 (2021) 176–183.
[65] C.F. Lu, X.Y. Yuan, L.Z. Li, W. Zhou, J. Zhao, Y.M. Wang, S.Q. Peng, Ecotoxicol. Environ. Saf. 122 (2015) 537–544.
[66] R. Merget, T. Bauer, H.U. Küpper, S. Philippou, H.D. Bauer, R. Breitstadt, T. Bruening, Arch. Toxicol. 75 (2002) 625–634.
[67] T. Skuland, M. Låg, A.C. Gutleb, B.C. Brinchmann, T. Serchi, J. Øvrevik, J.A. Holme, M. Refsnes, Part. Fibre Toxicol. 17 (2020) 13.
[68] T. Wu, S. Zhang, X. Liang, K. He, T. Wei, Y. Wang, L. Zou, T. Zhang, Y. Xue, M. Tang, Toxicol. Vitr.: Int. J. Publ. Assoc. BIBRA 56 (2019) 126–132.
[69] J. Liu, X. Feng, L. Wei, L. Chen, B. Song, L. Shao, Crit. Rev. Toxicol. 46 (2016) 348–384.
[70] A. Rodriguez-Garraus, A. Azqueta, A. Vettorazzi, A. López de Cerain, Nanomaterials 10 (2020).
[71] A. Scherzad, T. Meyer, N. Kleinsasser, S. Hackenberg, Materials 10 (2017).

[72] L. Bobyk, A. Tarantini, D. Beal, G. Veronesi, I. Kieffer, S. Motellier, E. Valsami-Jones, I. Lynch, P.-H. Jouneau, K. Pernet-Gallay, C. Aude-Garcia, S. Sauvaigo, T. Douki, T. Rabilloud, M. Carriere, Environ. Sci.: Nano 8 (2021) 806–821.
[73] S. Roy, Z. Liu, X. Sun, M. Gharib, H. Yan, Y. Huang, S. Megahed, M. Schnabel, D. Zhu, N. Feliu, I. Chakraborty, C. Sanchez-Cano, A.M. Alkilany, W.J. Parak, Bioconj. Chem. 30 (2019) 2751–2762.
[74] T. Xia, M. Kovochich, M. Liong, L. Mädler, B. Gilbert, H. Shi, J.I. Yeh, J.I. Zink, A.E. Nel, ACS Nano 2 (2008) 2121–2134.
[75] S. George, S. Pokhrel, T. Xia, B. Gilbert, Z. Ji, M. Schowalter, A. Rosenauer, R. Damoiseaux, K.A. Bradley, L. Mädler, A.E. Nel, ACS Nano 4 (2010) 15–29.
[76] M. Horie, Y. Tabei, Free Radic. Res. (2020) 1–12.
[77] A. Nel, T. Xia, L. Mädler, N. Li, Science 311 (2006) 622–627.
[78] B. Das, S. Tripathy, J. Adhikary, S. Chattopadhyay, D. Mandal, S.K. Dash, S. Das, A. Dey, S.K. Dey, D. Das, S. Roy, J. Biol. Inorg. Chem.: JBIC: a Publ. Soc. Biol. Inorg. Chem. 22 (2017) 893–918.
[79] C.-c Jiang, Y.-k Cao, G.-y Xiao, R.-f Zhu, Y.-p Lu, RSC Adv. 7 (2017) 7531–7539.
[80] S.J. Soenen, W.J. Parak, J. Rejman, B. Manshian, Chem. Rev. 115 (2015) 2109–2135.
[81] N. Feliu, D. Docter, M. Heine, P. del Pino, S. Ashraf, J. Kolosnjaj-Tabi, P. Macchiarini, P. Nielsen, D. Alloyeau, F. Gazeau, R.H. Stauber, W.J. Parak, Chem. Soc. Rev. 45 (2016) 2440–2457.

Naouale El Yamani, Ph.D. Senior scientist at (NILU). She has more than 10 years' experience in genetic toxicology, *in vitro* studies and NAMs, nanotoxicology, cellular toxicology, human biomonitoring, human hazard and risk assessment, data handling and statistics, human hazard and risk assessment. Validation and harmonization of high throughput (HTP) test methods as well as adaptation and implementation of new OECD TGs more suitable for nanoparticles. Member of EEMGS, NPST, EuroTOX and ICAWG societies and serves as peer journal reviewer for Mutation research, Genetic toxicology and Environmental molecular mutagenesis and Nanomaterial Journals. Reviewer Board Member for Nanomaterials.

Espen Mariussen, Dr Sci, ERT registered toxicologist. Senior researcher at the public health Institute FHI. Extensive experience in toxicology and environmental chemistry. Expertize in neurotoxic, immunotoxic and ecotoxic effects of toxicants, which includes organo-halogen compounds, heavy metals, emission gasses, chemical warfare agents and nanoparticles. Experience in techniques in cellular biology for mechanistic research, analytic chemistry and handling animals such as rats, mice and fish. Member of the national committee for approval of European registered toxicologists (ERT). 70 publications in peer reviewed journals and book chapters.

Maria Dusinska, Ph.D., research professor (DSc.), ERT registered toxicologist. Senior scientist and director of a GLP at NILU. More than 35 years of experience in the fields of environment and health, advanced in vitro models, development and validation of NAMs, mechanisms of toxicity (MoA) of environmental and industrial pollutants, mutagenicity and carcinogenicity, hazard and risk assessment, nanosafety, DNA damage and repair. Member of the OECD expert group for genetic toxicology and nanotoxicology, member of the Scientific Committee on Consumer Safety (SCCS), member of the ISO/TC229 on nanotechnology and cross-cutting working group on genotoxicity in EFSA. Coordinates H2020 NMBP13 project RiskGone (2019–2023, https://riskgone.wp.nilu.no/). More than 350 publications in peer reviewed journals.

Elise Rundén-Pran, Ph.D. ERT registered toxicologist. Senior scientist and Section leader at NILU. She has more than 20 years' experience in toxicology, hazard and risk assessment, and advanced in vitro cellular models. Expertize in Adverse outcome pathways and underlying mechanisms of cellular degeneration in advanced in vitro/ex vivo models, human risk assessment and regulatory toxicology for approval and safety labeling of pesticides in Norway.Executive officer at the Norwegian agricultural inspection service, Pesticide section. Member of the Norwegian ERT committee for approval of ERT toxicologists and the Norwegian Scientific committee for food and environment. 35 scientific papers in peer review journals.